Chapter 19

Tracking Odorant Plumes

Matthew A. Reidenbach

Abstract

Chemical signals are primarily distributed throughout aquatic environments by processes that are affected by turbulence. Turbulence continually stirs and mixes chemical odorants into complex, filamentous structures that are sampled by organisms. These odorant signals are critical for survival and/or reproductive success of most aquatic animals, and the time varying spatial structure of velocity and concentration offers valuable guidance cues while navigating in a plume. Two separate techniques are described to simultaneously measure a turbulent odor plume on a scale relevant to the chemosensors and mechanosensors located along the antennules of aquatic organisms. The first, planar laser induced fluorescence (PLIF), is used to quantify odorant concentrations, while the second, particle image velocimetry (PIV), is used to measure turbulent fluid velocities.

Key words Planar laser induced fluorescence, Particle image velocimetry, Odor plumes, Turbulence, Olfaction, Chemoreception

1 Introduction

Chemical signals are crucial to aquatic organisms for feeding, reproduction, predator avoidance, or, in the case of sessile animals, larval determination of substrate choice [1]. The dispersal of chemicals in the aquatic environment occurs primarily by gross advection of the water mass and by localized turbulent eddies. The movement of odor signals in water and their distribution patterns, accordingly, are inextricably linked with the hydrodynamic features responsible for dispersal, and comprise a critical part of the sensory environment [2, 3]. Many animals actively sample dissolved odorants in a fluid using appendages bearing arrays of hair-like chemosensory sensilla. These animals sample their surrounding odor and fluid environment by flicking their appendages, essentially taking a "sniff" [4–6]. The frequency of this flicking behavior, the size of the appendage, and arrangement and density of sensors all likely play a role in the kind of information an animal can extract from the plume [2, 7].

Fabio Marques Simoes de Souza and Gabriela Antunes (eds.), *Olfactory Receptors: Methods and Protocols*, Methods in Molecular Biology, vol. 1820, https://doi.org/10.1007/978-1-4939-8609-5_19,

Turbulence within the flow continually stirs and mixes chemical odorants into complex, filamentous structures. These filaments are composed of discrete packets of odor that are surrounded by little to no odor [8]. The spatial and temporal structure of these odor filaments within a plume offers valuable information on source location [4, 9]. However, odor information alone does not appear to provide enough information to organisms to undergo effective search strategies [1]. Although the scalar and hydrodynamic structure of odor plumes is well documented [10, 11], the instantaneous chemical and flow information available to organisms on the scale relevant to their sensory organs is not well understood [3].

Here, two techniques are described to quantify the spatial concentration and velocity structure on the scale of a turbulent plume, O(m), down to the scale relevant to the chemosensors and mechanosensors located along the sensory organs of organisms, O(μm). A planar laser induced fluorescence system (PLIF) is used to measure the spatial and temporal structure of chemical concentrations in an odorant plume, while particle image velocimetry (PIV) provides both spatial and temporal information of fluid velocities within the plume. A method to combine these two techniques to simultaneously quantify chemical concentrations and velocity fields within a plume is described. The spatial resolution offered by this dual technique is key, since it provides information relevant to what is sampled on often the spatially distributed array of olfactory and mechanoreceptors. Although many PLIF and PIV systems can be separately purchased as a single integrated system, the prices often range from the tens to hundreds of thousands of dollars. The materials and methods described here will enable the user to construct their own systems at a substantially reduced cost.

2 Materials

The techniques described here are primarily laboratory based and therefore some experimental test facility that can hold and create water movement is necessary. This can range anywhere from a large water flume (Fig. 1) to a small test chamber that can fit under a microscope. When conducting PLIF, a fluorescent dye is needed that emits fluoresced light under an applied laser light. These dyes absorb a portion of the excitation energy and re-emits a portion of the absorbed energy as fluorescence [12]. There are numerous organic fluorescent dyes that can be used, but two common dyes are fluorescein, which has a peak light absorption at 490 nm and a peak emission wavelength maximum of approximately 520 nm, and rhodamine 6G, which has a peak absorption of 525 nm and a peak emission of 555 nm. Therefore, in order to use fluorescein, a laser with a light emission at or near 490 nm is necessary. Typically

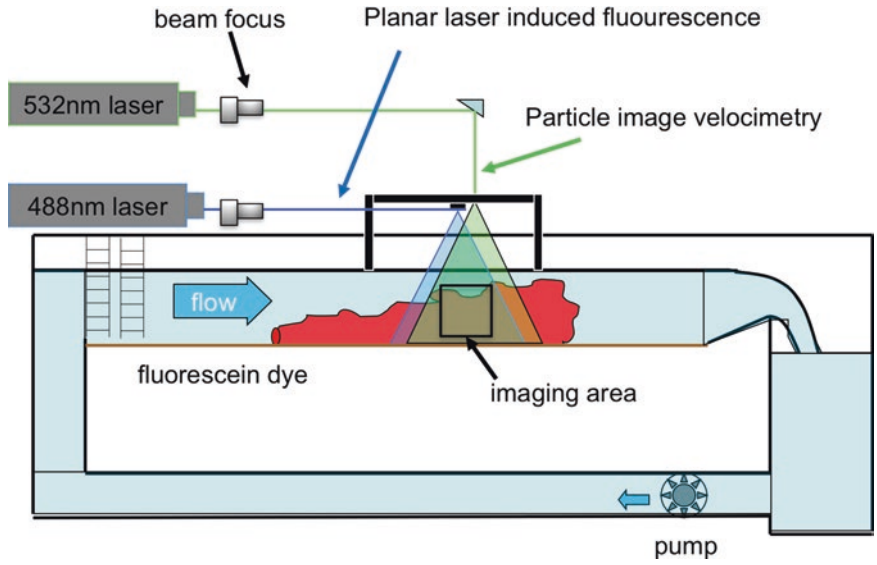

Fig. 1 Schematic of recirculating water flume. Fluorescein dye is injected in to the bulk flow. A coupled PLIF/PIV system is shown that consists of two lasers, a 488 nm laser to conduct planar laser induced fluorescence and a 532 nm laser for particle image velocimetry. The PLIF laser is first passed through a beam focus (if necessary) and then to a scanning mirror to illuminate a light sheet, while the PIV laser passes through a beam focus to a convex lens to create a light sheet. As the dye with particles passes through the imaging area, the lasers are scanned or pulsed at alternating times and sequential images are taken

a continuous wave (CW) argon-ion laser that emitts a blue laser beam (emission between 470 nm and 490 nm) is used. For Rhodamine 6G, an argon-ion laser that emitts at 514.5 nm can be used. These lasers should output a beam that is close to a Gaussian cross section and have stable power output.

Many odors detectable by aquatic organisms are composed of amino acids with a molecular diffusivity, $D = 1 \times 10^{-9}$ m^2 s^{-1}. Fluorescein dye has a $D = 0.51 \times 10^{-9}$ m^2 s^{-1}, while Rhodamine 6G has a $D = 1 \times 10^{-9}$ m^2 s^{-1}, making either a good choice as a surrogate to model odor transport. For reasons described later in the methods, if a combined PLIF-PIV system is required, it is recommended that fluorescein dye and a blue laser (emission between 470 nm and 490 nm) be used. For the PIV system, a laser that emits at any wavelength can conceivably be applied. However, if a combined PLIF-PIV system is required, it is recommended that a green laser (emission at 532 nm) is used such that the wavelength emission is outside the range that would be absorbed by fluorescein dye.

2.1 Planar Laser Induced Fluorescence

1. Fluorescent dye: fluorescein.
2. Laser: Argon-Ion laser that emits light at or near 490 nm. The stronger the power the greater the intensity of light that will be

emitted from the dye. Typical PLIF lasers have light emission power ratings of 100 mW to 1 W or greater.

3. Laser goggles for eye protection at light emitting wavelengths.
4. Scanning mirror: A computer-controlled scanning mirror (such as a moving-magnet scanning mirror) is used to scan the laser light at an equal intensity across the imaging area (*see* **Note 1**).
5. CCD camera: A CCD camera that has computer-controlled triggering to image the emitted light from the dye. The correct camera to use is a trade-off between light sensitivity, bit-depth, and framing rate. Cameras with low light capabilities and higher pixel counts often produce better images. Monochrome and color cameras can both work, but monochrome is preferred since image size is minimized (*see* **Note 2**).
6. Camera lens: Most commercially available lenses that can attach to the camera will work, but it is best to use a flat-field lens that has good low light capabilities with large aperture openings (*see* **Note 3**).
7. Laser beam focus: If necessary, optics to focus a laser beam can be placed between the laser and scanning mirror to reduce the diameter of the beam and create an optically thin light sheet at the imaging area.
8. Lens filter: To enhance the imaging and remove ambient light from the CCD images it is helpful to utilize either a bandpass or longpass filter, attached to the camera lens. If a combined PLIF/PIV system is used, a 520 nm longpass filter is recommended.
9. Computer with instrument control software and hardware: A laptop or desktop computer with instrument controls (such as LabView®) to enable image triggering and acquisition and scanning mirror control at the correct time.

2.2 Particle Image Velocimetry

1. Seeding particles: These should be neutrally buoyant in water and highly reflective. They can be made out of a variety of substances, included glass beads, polystyrene, and polyethylene. A common choice of particles for use in water are silver coated hollow glass spheres at approximately a 10 μm diameter.
2. Laser: Since the PIV laser needs to just illuminate the seeding particles, there are many options, including pulsed Nd:YAG lasers, argon-ion lasers, or laser diodes. Laser diodes are typically the cheapest but provide a continuous, lower-intensity beam of laser light as compared to short, intense pulses of light provided by Nd:YAG lasers. If a dual PLIF-PIV system is used, it is recommended that a 532 nm laser be used.
3. Laser goggles for eye protection.

4. Convex lens: This lens is used to spread the laser beam in to a sheet of light. They are typically categorized in the degree that they spread the beam, with larger degrees creating a wider sheet.
5. CCD camera: The same camera as described in Subheading 2.1 for PLIF can be used for PIV. If the camera is just being used for PIV, an 8-bit camera will typically be fine.
6. Lens filter: A bandpass filter that only allows the emitted light from the illuminated particles to be imaged. If a combined PLIF-PIV system is used, it is necessary to use a 520 nm long-pass filter. This filter blocks ambient light from the PLIF laser (typically a 488 nm argon-ion laser), but allows imaging of the PIV particles from the 532 nm laser.

3 Methods

3.1 Planar Laser Induced Fluorescence, Setup and Calibration

1. Measure and mix the fluorescein dye to the required concentration (*see* **Note 4**). The concentration to use depends upon the strength of the laser light and sensitivity of the camera (*see* **Notes 5–9**). The correct concentration should use the full dynamic range of the camera's imaging capabilities, from near-saturation of light at highest concentrations to near-dark at low concentrations.
2. Align the laser through the focusing optics to reduce the beam diameter, and then to the scanning mirror. Using the computer controls, adjust the range of the scanning mirror so it sweeps the laser across an arc to illuminate the entire imaging area.
3. A small concentration of dye needs to be well mixed within the experimental chamber to create a uniform amount of background emitted light. Typically, for a 12-bit camera (gray scale values from 0 to 4095) the background should have a light intensity of approximately 200.
4. Release dye in to the imaging area and sweep the laser one or more times using the scanning mirror to create a light sheet. While the sweep is in process, acquire an image of the fluoresced light. The integration time of the image needs to be short enough to prevent distortion of the image, but long enough to capture enough fluoresced light from the dye (*see* **Note 10**).
5. Perform a calibration between the light emitted from the fluoresced dye to the pixel light intensity of the acquired image. First, image the fluoresced light from the full concentration of the dye and then, subsequently image dilutions of the dye at lower concentrations (*see* **Note 11**). A linear-fit between light intensity and dye concentration should be found. Typically, 3 or more concentrations should be measured to conduct the linear fit.

6. Image processing: Raw PLIF images are processed to remove biases in the data, including varying pixel dark response, varying pixel response to fluorescence intensity, and laser attenuation due to the background dye concentrations [12]. The method for processing includes taking a dark image, D, of light levels with the lens cap on the camera, a background, B, of well-mixed background dye concentration, and a raw PLIF image, RI (Fig. 2).

$$C(i,j) = b\frac{\mathrm{RI}(i,j) - B(i,j)}{B(i,j) - D(i,j)} \tag{1}$$

$C(i,j)$ is the light intensity at pixel location i, j and b is the average background intensity of the dye. C is then computed as light intensity (for a monochrome 12-bit camera, these are gray scale values from 0 to 4095), that can be converted to dye concentration through the previously performed calibration between concentration and light intensity.

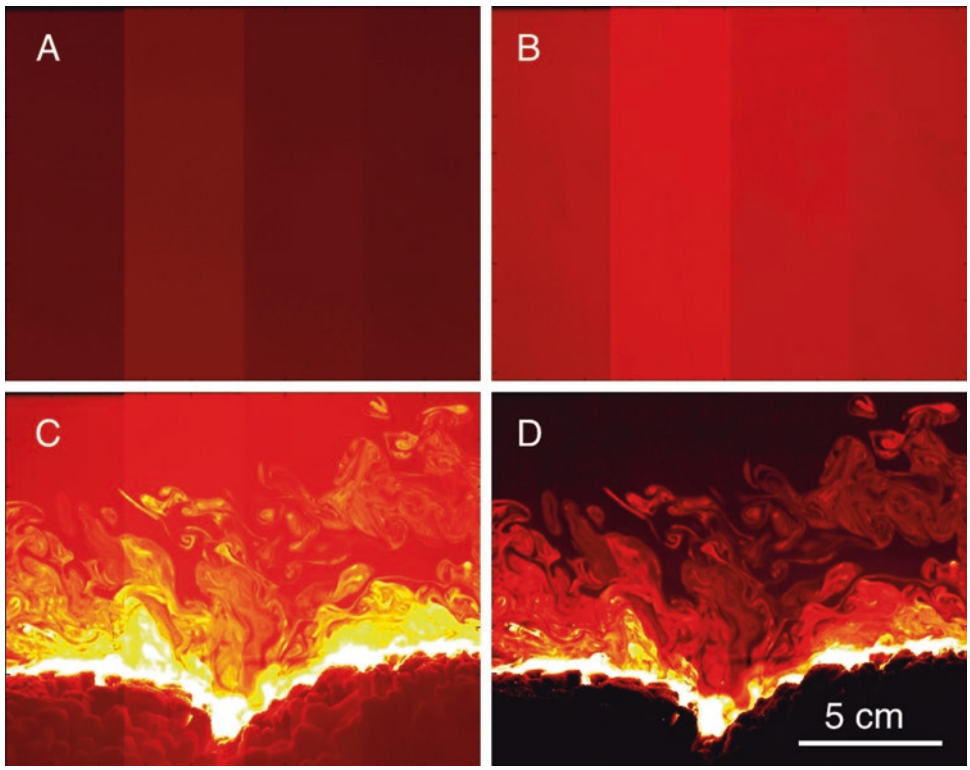

Fig. 2 Sequence of images used to process PLIF images to remove biases in the data. (**a**) ***D*** = dark image taken with the lens cap on, (**b**) ***B*** = background image taken of the well-mixed background dye concentration, (**c**) ***RI*** = raw Image, and (**d**) ***PI*** = processed image. Final processed image shows dye released from a coral surface, with color intensity proportional to dye concentration

3.2 Particle Image Velocimetry, Setup and Calibration

1. Add particles to the water in the flume and mix thoroughly to obtain an even suspension. Seeding density should provide approximately 5–10 particles per the smallest subaveraging window [13], which is the scale at which velocities are estimated (typically 16 × 16 pixels in dimension).
2. Align the PIV laser beam through focusing optics and then through the convex lens to create a light sheet that is slightly wider than the imaging area. Various imaging areas can be employed that typically range from 1 cm by 1 cm, up to 30 cm by 30 cm. If a dual PLIF/PIV system is required, the PIV laser-light sheet should directly overlap and illuminate the same 2-dimensional plane as the PLIF laser-light sheet. Micro-PIV systems can measure at much smaller scales, but typically require fluorescent particles as well as specialized optics [14].
3. Create a square grid (Fig. 3) and place it within the laser sheet. Image the grid so that a conversion of pixel to area dimension of the image can be performed (*see* **Note 12**).
4. If a continuous laser is being used (*see* **Note 13**), sequential images need to be captured to quantify displacement of the particles between image pairs. The correct time between images, Δt, will depend upon the water velocity and size of the image. This time, Δt, should be long enough to be able to image particle movements, but short enough to ensure that there is significant overlap of particles within each subaveraging window between successive images.
5. Images of particle trajectories should be analyzed using a numerical method that employs cross-correlation to calculate the displacement of particles over a given time period between image frames [13]. Many open-source PIV software analysis packages, along with tutorials, are available (e.g., MatPIV which is MATLAB® based).
6. Particle displacements between image pairs will be computed in pixel dimensions (*see* **Notes 14** and **15**). Utilizing the image of the grid, a conversion between particle displacement in pixel units to length can be computed (*see* **Note 16**). Knowing the time between images, Δt, velocity can then be quantified at the spatial scale of the smallest averaging subwindow and temporal scale of Δt (*see* **Note 17**). Many PIV software analysis packages perform this calculation for you.

3.3 Combined PLIF/PIV System

1. For the PLIF system, laser light with a wavelength of 488 nm (blue light) is emitted by an argon-ion laser.
2. The laser beam is focused using optics.
3. A light sheet is created using a scanning mirror. This sheet illuminates vertical plane through the water column parallel to the main flow direction.

Fig. 3 1 cm by 1 cm grid imaged within the light sheet, which is used to scale PIV images. This grid corresponds to the PIV and PLIF images shown in Fig. 4. Smaller or larger scale grids can be used depending upon the overall dimensions of the PLIF/PIV images

4. Fluorescent dye containing PIV particles is released upstream of the imaging area in to the bulk water flow (*see* **Note 18**). Within the bulk flow, a small amount of background dye, as well as PIV particles, are already well mixed.
5. As the dye passes through the laser light sheet, the fluoresced dye is imaged (*see* **Note 19**). The camera is fitted with a 520 nm optical long-pass filter, which blocks ambient laser light from the PLIF laser, but allows emitted light from the fluoresced dye to be imaged.
6. The laser sheet is scanned to illuminate the imaging field every Δt (or variable time period), with a wait period of equivalent to Δt (or other equivalent time period) after each scan. As an example, if 50 frames per second imaging occurs, $\Delta t = 0.02$ s; however, the time between successive PIV or PLIF images is $2\Delta t = 0.04$ s since PLIF and PIV images are alternately acquired.
7. For PIV imaging, a second laser with an output wavelength of light at 532 nm is used. The PIV laser is pulsed at $2\Delta t$ intervals at alternating time periods when the PLIF laser is not being scanned.
8. The PIV laser is pulsed through a cylindrical lens to create a light sheet, aligned along the same 2-dimensional plane as the PLIF laser.
9. Using the same camera as in the PLIF imaging, reflected light from the particles are illuminated and imaged at 532 nm. Since 532 nm is outside the absorption band of fluorescein, the PIV laser does not excite the fluorescein dye. Therefore, during the

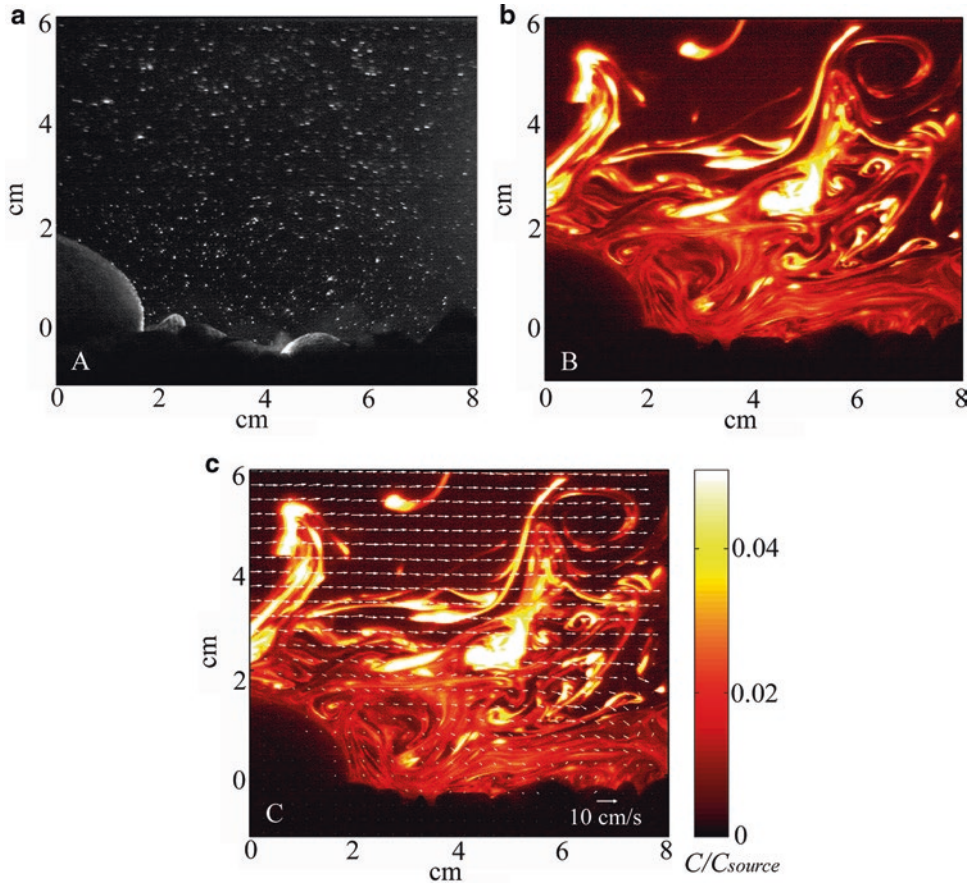

Fig. 4 The combined PLIF/PIV technique. (**a**) PIV image of flow over rough bed topography with particles added to the bulk water flow (**b**) PLIF image of plume structure taken 0.04 s after the PIV image. (**c**) Combined plume structure from PLIF and velocity vectors calculated from PIV cross-correlation analysis. Plume was created by emitting fluorescein dye 0.5 m upstream from the imaging area. Flow is from left to right

PLIF laser scan, only fluoresced dye is imaged, while during the PIV laser pulse, only particles are imaged (*see* **Note 20**).

10. PIV images are processed using MatPIV© or a similar PIV software program.
11. The final output from the software produces a horizontal and vertical estimate of particle displacements for every subwindow. Using the pixel to length conversion, and time between PIV images, $2\Delta t$, the fluid velocity can be computed.
12. Output of the combined PLIF/PIV technique provides overlapping estimates of plume and background flow velocities, along with dye concentrations (Fig. 4). These simultaneous measurements can be used to quantify the directional flux of chemicals [15] within a plume (*see* **Note 21**).

4 Notes

4.1 Planar Laser Induced Fluorescence

1. A cylindrical lens can be used in place of a scanning mirror, however this gives uneven light distribution in the static sheet which must be corrected for in post-processing.
2. The bit depth of the CCD camera determines light resolution, and a camera with a bit-depth N can resolve 2^N variations in light intensity. The framing rate sets the maximum rate at which images can be collected, while the sensitivity of the sensor determines how many light photons are needed to initiate a pixel response. Higher sensitivity cameras can operate better in low light conditions.
3. Flat-field lenses are preferred in PLIF and PIV applications, since spherical lenses distort images at the edges.
4. Fluorescein dye has a low sensitivity to temperature changes; however, the absorption spectra of fluorescein is strongly dependent on pH [12], and is susceptible to photo-bleaching [16].
5. Trial and error will likely be needed in order to determine the correct concentration for experiments given that the measurement location for PLIF may be substantially downstream from the release point, and thus concentrations may be much lower.
6. If too high a concentration of dye is used, it can attenuate the laser beam within the imaging area. Likewise, if too high an intensity of laser light is used, a non-linear relationship between dye concentration and emitted light may occur.
7. Care must be taken to ensure that the dye solution at the source is at the same temperature as the water used in the experimental facility, otherwise density differences will alter the buoyancy of the plume.
8. If necessary, the dye can be embedded in to a gelatin solution and a gel type mixture can be produced that can be coated on to surfaces [17].
9. If odors are used in the source, their concentrations should be measured relative to dye concentrations and then a conversion from dye concentration to odor concentration can be performed.
10. A plume that is being advected through the imaging area can be distorted if the image integration timescale relative to advection timescale is too long. In these instances, a scanning mirror that provides a dynamic scan of the image area can improve image quality.
11. Imaging at multiple locations downstream might be necessary if large scale quantification of plume dynamics is needed.

4.2 Particle Image Velocimetry

12. Care should be taken to place the grid used to compute the size of the image directly within the sheet of the laser. Since the depth of field of the image is small, any out-of-plane imaging of the grid could substantially alter results.
13. Either pulsed or continuous lasers can be used for PIV. Pulsed lasers, such as Nd:YAG, often generate much greater light intensity over short periods. This enhances the sharpness of the images, especially for particle motions in fast flows, however the timing of the image acquisition relative to the laser pulse often becomes difficult.
14. Removal of particulates in the water by filtration before adding the PIV seeding can improve image quality by ensuring only neutrally buoyant, highly reflective PIV particles are illuminated.
15. Getting the seeding density correct is important for good data quality. Typically, 5–10 particles in the smallest subaveraging window is ideal. As long as individual particles can be easily identified within the acquired image, it is better to have more seeding than less. However, care should be taken not to overseed such that it alters the properties of the flow.
16. If light reflectance from the particles is uneven, the algorithm which computes velocities can be biased by the highly reflective particles. An intensity-capping algorithm can be implemented which can improve cross-correlation PIV results [18].
17. Accuracy of the PIV measurements can be estimated either using a separate flow sensor (such as an acoustic Doppler velocimeter) or using a calibration facility where the velocity of the flow is known. The accuracy of the velocity measurements in PIV is usually found to be relative to the magnitude of the mean velocity [19].

4.3 Combined PLIF/PIV

18. Particles and dye must be mixed together in the source solution and care should be made to get PIV particle concentrations in the source solution equal to the concentrations in the bulk flow.
19. If studying flows in a large-scale water flume, it may be necessary to pass the laser sheets through a glass window insert suspended over the flume that contacts the water surface. This minimizes the laser diffraction caused by small ripples on the water surface.
20. The magnitude of the distortion within the PIV and PLIF images will depend upon the integration time of the image relative to the ambient velocity of the fluid. Likely the optimal integration time will be a trade-off between acquiring enough light in the image and minimizing the blurring of either dye or particles.

21. Once PIV and PLIF images have been collected and processed, velocity data will be spatially separated on the distance of the smallest subaveraging window (typically 16 by 16 pixels), while concentration data from PLIF images will be at the individual pixel level. Either the PIV data will need to be down-sampled or the PLIF data will need to be averaged over the subaveraging area window to enable PIV and PLIF data to be directly mapped on to one another.

Acknowledgments

This work was supported by National Science Foundation grants IIS-631864 and CBET-0933034 to M.A.R.

References

1. Webster DR, Weissburg MJ (2009) The hydrodynamics of chemical cues among aquatic organisms. Annu Rev Fluid Mech 41:73–90
2. Moore P, Crimaldi JP (2004) Odor landscapes and animal behavior: tracking odor plumes in different physical worlds. J Mar Syst 49:55–64
3. Mellon D, Reidenbach MA (2011) Fluid mechanical problems in crustacean active chemoreception. In: Barth FG, Humphrey JAC, Srinivasan MV (eds) Frontiers in sensing systems. Springer-Verlag, Wien, pp 159–170
4. Koehl MAR (2011) Hydrodynamics of sniffing by crustaceans. In: Breithaupt T, Theil M (eds) Chemical communication in crustaceans. Springer-Verlag, New York, pp 85–102
5. Nelson JM, Mellon D, Reidenbach MA (2013) Effects of antennule morphology and flicking kinematics on flow and odor sampling by the freshwater crayfish, *Procambarus clarkii*. Chem Senses 38(8):729–741
6. Waldrop LD, Reidenbach MA, Koehl M (2015) Flexibility of crab chemosensory sensilla enables flicking antennules to sniff. Bio Bull 229(2):185–198
7. Reidenbach MA, Koehl MAR (2011) The spatial and temporal patterns of odors sampled by lobsters and crabs in a turbulent plume. J Exp Biol 214:3138–3153
8. Crimaldi JP, Wiley MB, Koseff JR (2002) The relationship between mean and instantaneous structure in turbulent passive scalar plumes. J Turb 3(014):1–24
9. Atema J (1996) Eddy chemotaxis and odor landscapes: exploration of nature with animal sensors. Bio Bull 191:129–138
10. Atema J (1995) Chemical signals in the marine environment: dispersal, detection, and temporal signal analysis. Prod Nat Acad Sci 92(1):62–66
11. Crimaldi JP, Koseff JR (2001) High resolution measurements of the spatial and temporal scalar structure of a turbulent plume. Exp Fluids 31(1):90–102
12. Crimaldi JP (2008) Planar laser induced fluorescence in aqueous flows. Exp Fluids 44:851–863
13. Sveen JK, Cowen EA (2004) Quantitative imaging techniques and their application to wavy flows. World Scientific Pub. Co., Singapore
14. Devasenathipathy S, Santiago J, Wereley S, Meinhart C, Takehara K (2003) Particle imaging techniques for microfabricated fluidic systems. Exp Fluids 34(4):504–514
15. Reidenbach MA, Limm M, Hondzo M, Stacey MT (2010) The effects of bed roughness on boundary layer mixing and mass flux across the sediment-water interface. Water Resour Res 46:7. https://doi.org/10.1029/2009WR008248
16. Ferrier AJ, Funk DR, Roberts PJW (1993) Application of optical techniques to the study of plumes in stratified fluids. Dyn Atmos Oceans 20:155–183

17. Reidenbach MA, Koseff JR, Monismith SG (2007) Laboratory experiments of fine-scale mixing and mass transport within a coral canopy. Phys Fluids 19(7):075107
18. Shavit U, Lowe RJ, Steinbuck JV (2007) Intensity capping: a simple method to improve cross-correlation PIV results. Exp Fluids 42(2):225–240
19. Reidenbach MA, George NT, Koehl MAR (2008) Antennule morphology and flicking kinematics facilitate odor sampling by the spiny lobster, *Panulirus argus*. J Exp Biol 211:2849–2858